

First-Principle Calculation of the Electronic Structure of Sb-Doped SrTiO₃

Yun Jiangni^{1,†}, Zhang Zhiyong¹, Deng Zhouhu¹, and Zhang Fuchun^{1,2}

(1 Institute of Information Science and Technology, Northwest University, Xi'an 710069, China)

(2 College of Physics & Electronic Information, Yan'an University, Yan'an 716000, China)

Abstract: The electronic structure, including band structure, density of states (DOS), and partial density of states of SrTi_{1-x}Sb_xO₃ with $x=0, 0.125, 0.25$, and 0.33 is calculated from the first principles of plane wave ultrasoft pseudo-potential technology based on density function theory. The calculated results reveal that due to the electron doping, the Fermi level moves into the conduction bands for SrTi_{1-x}Sb_xO₃ with $x=0.125$ and the system shows metallic behavior. In addition, the DOS moves towards low energy and the optical band gap is broadened. The wide band gap and the low density of the states in the conduction band result in the transparency of the films.

Key words: first principles; SrTiO₃; Sb-doping; electronic structure; transparent films

PACC: 7115B; 7115H; 7115J

CLC number: TN304.02

Document code: A

Article ID: 0253-4177(2006)09-1537-06

1 Introduction

Strontium titanate (SrTiO₃), a typical perovskite material, is of great interest for its fundamental research and potential applications in ferroelectricity, grain-boundary barrier layer capacitors, oxygen-gas sensors, epitaxial growth substrates for high temperature superconductor thin films, and optical switches^[1~4]. It is well known that stoichiometric SrTiO₃ is a good insulator with a band gap of about 3.2eV at room temperature. But its conductivity can be induced either through the reduction of oxygen (SrTiO_{3-x}) or through impurity doping, which has important applications in oxide devices^[5] as well as in the theoretical and experimental investigations of SrTiO₃^[6~10].

The behavior of doped SrTiO₃ has been widely studied in an attempt to understand the rich variations in physical properties arising from carrier doping^[8~12]. The effects of Sc and V impurities and O vacancies on the electronic properties have been studied by Luo *et al.*^[11] using *ab initio* pseudo-potential density function theory. Takeshi *et al.*^[12] have experimentally found that the metal-insulator transition appears in Nb-doped SrTiO₃ when the doping concentration is increased. Our group studies impurity doping in SrTiO₃ using Sb as a substi-

tuting element in order to obtain a useful material for oxide superlattice and junction applications. Since Sb is a semimetal, a different behavior for Sb-doped SrTiO₃ is expected from that of other metal-doped SrTiO₃. In the case of SrTi_{1-x}Sb_xO₃, however, there has been little theoretical work on the electronic structures for different x values. It is necessary for one to use the first-principles method to explore the effect of Sb doping on the electronic structure.

In this paper, we perform first-principle calculations of the electronic structure of SrTi_{1-x}Sb_xO₃ for the cases of $x=0, 0.125, 0.25$, and 0.33 with the CASTEP software package^[13] based on density function theory (DFT) using the supercell approach. Since the supercell approach is time-consuming, we construct a supercell of eight unit cells consisting of 40 atoms at most.

2 Theoretical model and calculational method

2.1 Theoretical model

SrTiO₃ has an ideal cubic perovskite structure at room temperature. It belongs to the space group Pm3m(O_h), with the Sr atom sitting at the origin, Ti at the body center, and three oxygen atoms at

†Corresponding author. Email:yunjiangni821001@sohu.com

the three face centers, and its lattice constant is $a = b = c = 0.3905 \text{ nm}$. In our calculation, the theoretical model is shown in Fig. 1.

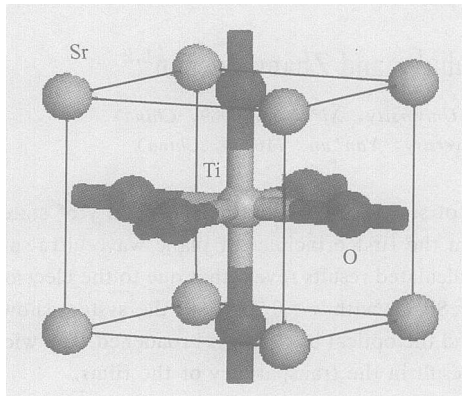


Fig. 1 Model of cubic SrTiO_3

2.2 Computational method

All of the calculations in this paper were performed using the CASTEP software package in Material Studio 3.2. CASTEP is a quantum mechanics program based on density functional theory (DFT). It uses the plane-wave pseudo-potential approach; the particle-field interaction is substituted by a pseudo-potential, electronic wavefunctions are expanded in terms of a discrete plane-wave basis set, and the exchange and correlation potential are described with the local-density approximation (LDA) and generalized gradient approximation (GGA), which are the most precise methods used for the calculation of electronic structure at present^[13,14].

In the present calculation, the pseudo-potential based on the GGA is employed. The cutoff energy of a plane-wave is set at 340 eV ; the maximum root-mean-square convergent tolerance is less than $2 \times 10^{-5} \text{ eV/atom}$; that is, the force imposed on each atom is not greater than 0.1 eV and 0.1 GPa for stress. The Brillouin zone integrations are approximated using the special k -point sampling scheme of Monkhorst-Pack and a $6 \times 6 \times 4$ k -point grid is used. All energy calculations are performed in reciprocal space.

3 Results and discussion

3.1 Electronic structure of undoped SrTiO_3

In order to show the Sb doping effect on the electronic structure of SrTiO_3 , the band structure,

total density of states (DOS), and partial density of states (PDOS) of stoichiometric SrTiO_3 are calculated first for comparison. The calculational results are shown in Figs. 2 and 3.

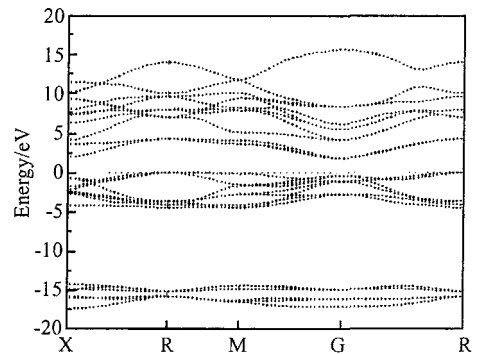


Fig. 2 Band structure of SrTiO_3

As shown in Figs. 2 and 3, the valence bands (VBs) of SrTiO_3 can be divided into two main zones: a lower valence band zone ($-17.6 \sim -13.8 \text{ eV}$) and an upper one ($-5.0 \sim 0.0 \text{ eV}$). The upper VB zone with nine bands consists mainly of $\text{O}2\text{p}$ states and has a bandwidth of about 5.0 eV . These values are consistent with the values of $5 \sim 6 \text{ eV}$ obtained by XPS^[15] and the FP-LAPW method in Ref. [16]. Below the $\text{O}2\text{p}$ states, $\text{Sr}4\text{p}$ and $\text{O}2\text{s}$ states form the lower VB zone. The other two VBs, at -33 and -56 eV , are not considered because their interaction with the two main mentioned VBs is weak. The most prominent unoccupied energy bands among the bottommost conduction bands (CBs) are mainly composed of the threefold degenerate $\text{Ti}3\text{d } T_{2g}$ states and twofold degenerate $\text{Ti}3\text{d } E_g$ states. Our calculated electronic structures of SrTiO_3 are consistent with the experimental results from scanning transmission electron microscopy, vacuum ultraviolet spectroscopy, and spectroscopic ellipsometry^[17].

There is an energy gap between the occupied $\text{O}2\text{p}$ states and the unoccupied $\text{Ti}3\text{d}$ states, which means that the SrTiO_3 is an insulator with a $\text{Ti}3\text{d}^0$ electron configuration. The value of the band gap is about 1.6 eV , which is smaller than the experimental value of about 3.2 eV and the value of about 1.8 eV with the LMTO-ASA method in Ref. [18]. The reason for this disagreement is the well-known shortcoming of the theoretical frame of DFT-LDA^[19].

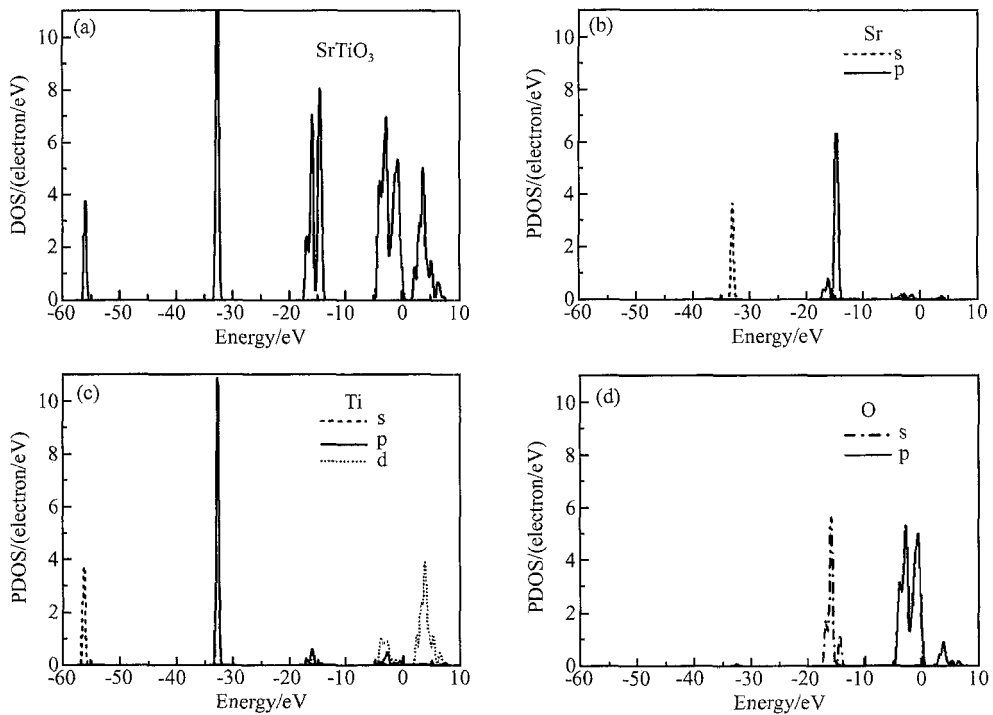


Fig. 3 DOS and PDOS of SrTiO₃. Fermi level is set to zero on the energy scale, the same as below.

3.2 Effect of Sb doping on the electronic structure

3.2.1 Single point energy

In our calculation, we take three Sb concentrations: SrTi_{0.875}Sb_{0.125}O₃, SrTi_{0.75}Sb_{0.25}O₃, and SrTi_{0.67}Sb_{0.33}O₃. First of all, we optimize the atomic coordinate of doped SrTiO₃ by CASTEP Geometry. Then the single point energy is calculated based on the optimized supercell model. The results are shown in Table 1.

Table 1 Single point energy of SrTi_{1-x}Sb_xO₃

Doping concentration	0	0.125	0.25	0.33
Supercell	2 × 2 × 2	2 × 2 × 2	2 × 2 × 1	3 × 1 × 1
Energy/ eV	- 3772.34	- 3787.23	- 3798.82	- 3810.31

The single point energy increases as the Sb doping concentration increases, which indicates that the Sb-doped SrTiO₃ is less stable. This is because the radius of Sb⁵⁺ (0.62nm) is smaller than that of Ti⁴⁺ (0.68nm), and the substitution of Sb⁵⁺ for Ti⁴⁺ results in crystal lattice aberration. Correspondingly, residual stress is generated in the process of crystallization, which causes repulsive interaction among redundant positive charges of

Sb⁵⁺. Therefore the single point energy increases. This case has also been discovered in Sr-doped In₂O₃^[20]. However, it should be noticed that the crystal structure of SrTiO₃ is still cubic perovskite.

3.2.2 Electronic structure of Sb-doped SrTiO₃

3.2.2.1 Density of states

Figure 4 shows the total DOS of SrTi_{1-x}Sb_xO₃ with $x = 0.125, 0.25,$ and 0.33 . Because the Sb doping introduces n-type carriers into the system^[21], the Fermi level goes into the CBs for $x = 0.125, 0.25$ and 0.33 , which is similar to that of Nb^[6] or V-doped^[11] SrTiO₃. At the same time, for the case of $x = 0.125, 0.25,$ and 0.33 , there is an additional peak below the lower VB zone, and the peak broadens with increased Sb doping. Below the upper VB zone, a peak with a bandwidth of about 1eV appears when $x = 0.125$. Two small peaks appear when $x = 0.25$, and these split into many peaks when $x = 0.33$. We will discuss these additional peaks later.

In addition, the DOS moves significantly towards lower energy and the optical band gap broadens with increased Sb doping concentration compared with the DOS reported in Fig. 3. The reasons are as follows: on one hand, the Burstein-Moss shift due to the high concentration of carriers

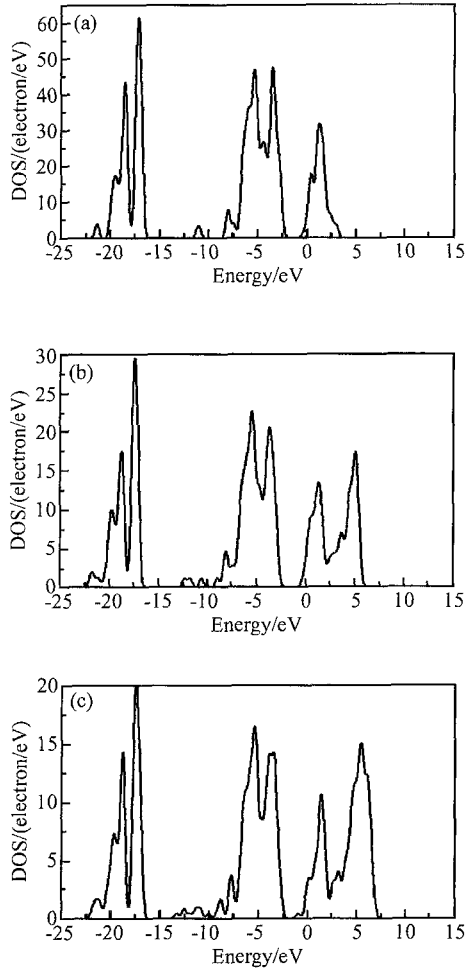


Fig. 4 DOS of $\text{SrTi}_{1-x}\text{Sb}_x\text{O}_3$ (a) $x=0.125$; (b) $x=0.25$; (c) $x=0.33$

makes the optical absorption edge move towards lower energy, and the optical band gap is broadened^[22]; on the other hand, interactions among electric charges result in a many-body effect, which causes the optical band gap to become narrow^[23]. But the Burstein-Moss effect on the band gap is more pronounced than that of the many-body effect, so the band gap broadens with increased Sb doping concentration.

It can be expressed by the following equation:

$$E_g = E_{g0} + E_g^{\text{BM}} - E_g^{\text{W}}$$

Here E_{g0} is the band gap of undoped SrTiO_3 , E_g^{BM} is the Burstein-Moss shift, and E_g^{W} is the change of conduction band resulting from the many-body effect among electrons. However, the band gap becomes smaller in cases of Nb-doped^[6] or V-doped^[11] SrTiO_3 .

In order to study the DOS quantitatively, the integrals of the DOS for SrTiO_3 with $x=0, 0.125,$

$0.25,$ and 0.33 are performed in the region with the energy -25eV to the Fermi level, and the results are 320, 313, 306, and 113 for $\text{Sr}_8\text{Ti}_8\text{O}_{24}$, $\text{Sr}_8\text{Ti}_7\text{SbO}_{24}$, $\text{Sr}_4\text{Ti}_3\text{SbO}_{12}$, and $\text{Sr}_3\text{Ti}_2\text{SbO}_9$, respectively. These values represent the number of electronic states that can be occupied by outer-shell electrons in the four systems. In our calculation, the valence states are $2s$ and $2p$ for O, $2s, 3p, 3d,$ and $4s$ for Ti, $4s, 4p,$ and $5s$ for Sr and $5s$ and $5p$ for Sb, indicating that the numbers of valence electrons are 6, 12, 10, and 5 for O, Ti, Sr, and Sb, respectively. Hence, in cases of SrTiO_3 with $x=0.125, 0.25,$ and 0.33 based on our supercell models, 320, 313, 306, and 113 valence electrons are included, respectively, which is in good agreement with the integral results. Comparing the number of electronic states that can be occupied with that of valence electrons, we can conclude that the VBs of $\text{Sr}_8\text{Ti}_8\text{O}_{24}$ are fully occupied and the Fermi level is just at the top of the VBs. The bottommost CBs of the three different Sb doping systems are fully occupied with electrons and the Fermi level moves into CBs. According to the conductive mechanism of semiconductors^[24], the conductivity of Sb-doped SrTiO_3 is greatly improved by the electrons provided by the Sb doping.

3.2.2.2 Partial density of states

Figure 5 shows the PDOS of $\text{SrTi}_{1-x}\text{Sb}_x\text{O}_3$ with different Sb doping amounts. There are many superfluous electrons in the bottom of the CBs and the Fermi level goes into the CBs, which indicates that the $\text{SrTi}_{1-x}\text{Sb}_x\text{O}_3$ shows the characteristics of a degenerate semiconductor. Also, the PDOS moves significantly towards lower energy with increased Sb doping concentration, and the dispersion of the CBs is aggravated due to the high doping concentration that makes the impurity atoms become closer to each other. In this case, the wave functions which are bounded by the doping ions greatly overlap, resulting in enhancement of the communication movement between the O2p orbit and the impurity atom orbit, so the valence band is broadened. In addition, the PDOS of doped SrTiO_3 has significant changes: One small peak emerges below the lower VB zone, to which the Sb5s state and O2s state contribute, and another peak appears near the bottommost of the upper VB zone, to which the Sb5s state and O2p state contribute. In particular, the two peaks broaden with increased doping concen-

tration.

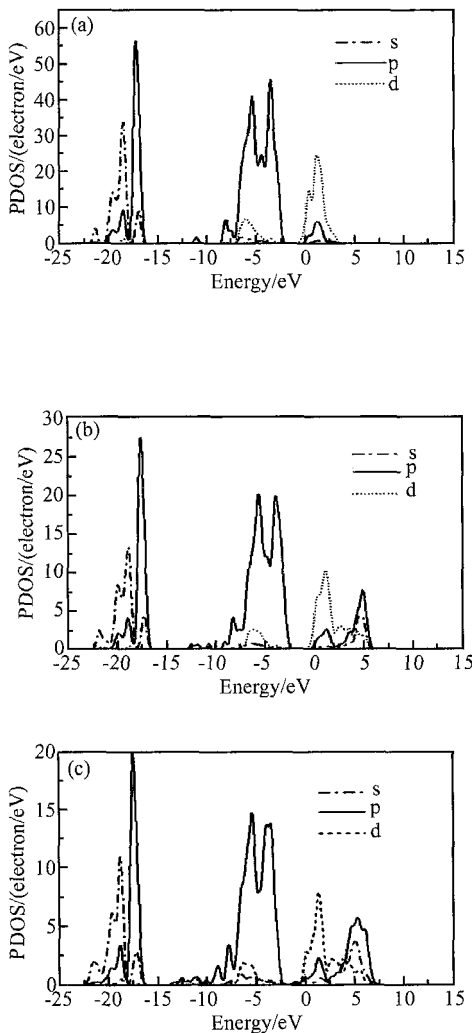


Fig.5 PDOS of SrTi_{1-x}Sb_xO₃ (a) $x = 0.125$; (b) $x = 0.25$; (c) $x = 0.33$

In turn to the CBs, it is highly dispersive and shows no localization characteristics with increased Sb doping. In our calculation, the PDOS in the Fermi level for Sr and Sb in the three different Sb doping systems are calculated. See Table 2. The Sb plays a more important role than the Sr in terms of contribution to the CBs. Therefore the Sb doping has a greater effect on the conductivity of SrTiO₃.

Table 2 Values of PDOS in the Fermi level with different Sb doping concentrations

Doping concentration	0.125	0.25	0.33
Sr (E_F)	0.035	0.179	0.106
Sb (E_F)	0.0083	0.201	0.233

4 Conclusion

In conclusion, we performed electronic struc-

ture calculations, including band structure, DOS, and PDOS, on SrTi_{1-x}Sb_xO₃ with $x = 0, 0.125, 0.25$, and 0.33 with first-principle calculations using plane wave ultra-soft pseudo-potential technology based on density function theory (DFT). Due to the electron doping, the Fermi level moves into the CBs for SrTi_{1-x}Sb_xO₃ with $x = 0, 0.125, 0.25$, and 0.33 , and these systems show metallic behavior. In addition, the DOS moves towards lower energy, and the optical band gap is broadened. The wide band gap and the low density of states in the conduction band result in the transparency of the films. Because of the absence of experimental results on the Sb-doped SrTiO₃ with different doping concentration, further experimental work is needed for comparison with our numerical results.

References

- [1] Li H C, Si W D, Alexander D W, et al. Thickness dependence of dielectric loss in SrTiO₃ thin films. *Appl Phys Lett*, 1998, 73(4) :464
- [2] Ernst F, Kienzle O, Ruhle M. Structure and composition of grain boundaries in ceramics. *J Eur Ceram Soc*, 1999, 19:665
- [3] Pradhana A K, Sahu D R, Roul B K, et al. Lanthanum-based manganite films on MgO using SrTiO₃ as a template layer. *J Appl Phys*, 2004, 96(2) :1170
- [4] Uedono A, Shimayama K, Kiyohara M, et al. Study of oxygen vacancies in SrTiO₃ by positron annihilation. *J Appl Phys*, 2002, 92(5) :2697
- [5] Suzuki S, Yamamoto T, Suzuki H, et al. Fabrication and characterization of Ba_{1-x}K_xBiO₃/Nb-doped SrTiO₃ all-oxide-type Schottky junctions. *J Appl Phys*, 1997, 81:6830
- [6] Guo X G, Chen X S, Sun Y L. Electronic band structure of Nb doped SrTiO₃ from first principles calculation. *Phys Lett A*, 2003, 317:501
- [7] Tokura Y, Taguchi Y, Okada Y, et al. Filling dependence of electronic properties on the verge of metal-Mott-insulator transition in Sr_{1-x}La_xTiO₃. *Phys Rev Lett*, 1993, 70:2126
- [8] Fujimori A, Hase I, Nakamura M, et al. Doping-induced changes in the electronic structure of La_xSi_{1-x}TiO₃: limitation of the one-electron rigid-band model and the Hubbard model. *Phys Rev B*, 1992, 46(15) :9841
- [9] Higuchi T, Tsukamoto T, Kobayashi K, et al. Electronic structure in the band gap of lightly doped SrTiO₃ by high-resolution X-ray absorption spectroscopy. *Phys Rev B*, 2000, 61(19) :12860
- [10] Evarestov R A, Piskunov S, Kotomin E A, et al. Single impurity in insulator: ab initio study of Fe-doped SrTiO₃. *Phys Rev B*, 2003, 67:064101-1
- [11] Luo W D, Duan W H, Steven G L, et al. Structural and electronic properties of n-doped and p-doped SrTiO₃. *Phys Rev B*, 2004, 70:214109-1
- [12] Tomio T, Miki H, Tabata H, et al. Control of electrical conductivity in laser deposited SrTiO₃ thin films with Nb doping. *J Appl Phys*, 1994, 76:5886

- [13] Segall M D, Lindan P J D, Probert M J, et al. First-principles simulation: ideas illustrations and the CASTEP code. *J Phys Cond Matt*, 2002, 14(11): 2717
- [14] Tetsuya Y, Hiroshi K Y. Physics and control of valence states in ZnO by codoping method. *Physica B*, 2001, 302-303: 155
- [15] Bocquet A E, Mizokawa T, Morikawa K, et al. Electronic structure of early 3d-transition-metal oxides by analysis of the 2p core-level photoemission spectra. *Phys Rev B*, 1996, 53: 1161
- [16] Cai M Q, Yin Z, Zhang M S. Optical properties of strontium titanate by ab initio calculation within density functional theory. *Chem Phys Lett*, 2004, 388: 2237
- [17] Van Benthem K, Elsasser C, French R H. Bulk electronic structure of SrTiO₃: experiment and theory. *J Appl Phys*, 2001, 90: 6156
- [18] Guo X G, Chen X S, Lu W. Optical properties of Nb doped SrTiO₃ from first principles study. *Solid State Commun*, 2003, 126: 441
- [19] Jones R O, Gunnarsson O. The density functional formalism, its applications and prospects. *Rev Mod Phys*, 1989, 61: 689
- [20] Sorescu M, Diamandescu L, Tarabasanur-Mihaila D, et al. Nanocrystalline rhombohedral In₂O₃ synthesized by hydrothermal and postannealing pathways. *J Mat Sci*, 2004, 39(2): 675
- [21] Wang H H, Chen F, Dai S Y, et al. Sb-doped SrTiO₃ transparent semiconductor thin films. *Appl Phys Lett*, 2001, 78(12): 1676
- [22] Burstein E. Anomalous optical absorption limit in InSb. *Phys Rev*, 1954, 93: 632
- [23] Mahan G D. Energy gap in Si and Ge: impurity dependence. *J Appl Phys*, 1980, 51: 2634
- [24] Huang K, Han R Q. *Solid state physics*. Beijing: Higher Education Press, 1988: 325

Sb 掺杂 SrTiO₃ 电子结构的第一性原理计算

贫江妮^{1,†} 张志勇¹ 邓周虎¹ 张富春^{1,2}

(1 西北大学信息科学与技术学院, 西安 710069)

(2 延安大学物理与电子信息学院, 延安 71600)

摘要: 计算了 Sb 掺杂 SrTi_{1-x}Sb_xO₃ ($x=0, 0.125, 0.25, 0.33$) 体系电子结构, 分析了掺杂对 SrTiO₃ 晶体的结构、能带、态密度、分波态密度的影响。所有计算都是基于密度泛函理论框架下的第一性原理平面波超软赝势方法。计算结果表明: 体系的导电性与掺杂浓度有关, Sb 掺杂在母体化合物 SrTiO₃ 中引入了大量的传导电子, 费米能级进入导带。当 Sb 掺杂浓度 $x=0.125$ 时, 体系显示金属型导电性。同时, 光学带隙展宽, 且向低能方向漂移, 可作为优良的透明导电薄膜材料。

关键词: 第一性原理计算; SrTiO₃; Sb 掺杂; 电子结构; 透明导电薄膜

PACC: 7115B; 7115H; 7115J

中图分类号: TN304.02

文献标识码: A

文章编号: 0253-4177(2006)09-1537-06

† 通信作者. Email: yunjiangni821001@sohu.com